

STUDY ON THE STABILITY OF RETAINED AUSTENITE IN MARINE STEEL

Received – Primljeno: 2019-09-24

Accepted – Prihvaćeno: 2019-11-20

Original Scientific Paper – Izvorni znanstveni rad

The residual austenite stability in marine steel was studied by different heat treatment processes. After heat-treatment process 1 (quenching + tempering) and heat treatment process 2 (quenching + intercritical annealing + tempering), the austenite content was determined by X-ray diffraction (XRD), and the microstructure of the test steel was tested by Scanning electron microscope (SEM), Transmission electron microscope (TEM), and Electron Backscattered Diffraction (EBSD). Experimental results showed that the microstructure of the test steel consisted of martensite/bainite + ferrite + retained austenite. The retained austenite volume fractions were 20,8 % and 18,1 %, respectively, for process 1 and process 2. The retained austenite morphology, C content, distribution, and grain size all affect a steel's thermal and mechanical stability. Film-like residual austenite with high C content and fine grain size has the best stability.

Key words: marine steel, heat treatment, microstructure, retained austenite, mechanical stability

INTRODUCTION

The overexploitation and consumption of abundant terrestrial and marine resources are the focus of mining in the world, whereas marine engineering materials need to cope with the harsh and complex marine environment. The use environment of marine engineering steel is generally harsh. It will be attacked by seawater, sea mud, and ocean atmosphere during service. The corrosion characteristics of different areas are also different. Therefore, steel for marine engineering should have high overall performance, such as excellent plasticity, impact toughness, weldability, and corrosion resistance [1-6]. It is believed that retained austenite stability is an important condition, affecting the ductility and low-temperature toughness of steel. Austenitic stability includes thermodynamic and mechanical stability.

For example, morphology, C content, grain size, and other factors will affect the stability of retained austenite. Retained austenite grain size affects thermodynamic stability. Retained austenite with high C content has higher stability. The distribution of retained austenite also affects a steel's mechanical properties. The use of different composition designs and heat treatment processes to organize retained austenite in steel has become a hot research topic.

In this work, a medium-manganese low-carbon steel of 0,1C – 2,44 Mn was subjected to (quenching + two-phase annealing + tempering) (QIT) and (quenching + tempering) (QT) heat-treatment processes to obtain high volume fractions of retained austenite. Residual

austenite and multiphase microstructures were characterized by SEM, TEM, EBSD, XRD.

MATERIALS AND METHODS

The experimental steel was smelted in a 200 kg vacuum-induction melting furnace with chemical composition (wt.%), Fe, 0,105C, 2,48Mn, 0,085Nb, 0,35Mo, 1,24Cu, 1,32Ni, and the steel ingot was heated and kept at 1 180 °C. The thickness of the blank was 115 mm, a 25-mm-thick hot rolled sheet was obtained after eight passes, and the final rolling temperature was 840 °C. After stratified water cooling, the red temperature was 350 °C. To determine the effect of different heat-treatment processes on retained austenite content and stability, the heat-treatment processes were used: process 1 (quenching + tempering) and process 2: (quenching + intercritical annealing + tempering). The rolled samples were taken onto a LINSEIS L78 RITA phase changer to determine the steady-state austenite transition start temperature of 701 °C and the austenite transformation end temperature of 762 °C. The test steel was austenitized at 850 °C for 10 min, quenched at 830 °C for 40 min, tempered at 640 °C for 40 min, and then air-cooled to room temperature, after which sample T1 was recorded. Another sample of experimental steel was austenitized at 850 °C for 10 min, quenched at 830 °C for 40 min, incubated at 720 °C for 50 min, then air-cooled to room temperature (intercritical annealing), tempered at 640 °C for 60 min, and air-cooled to room temperature again. The sample was recorded as T2. The microstructure was observed under EVO MA10 scanning electron microscopy (SEM) at a position halfway through the steel plate after grinding and polishing with 4 % nitric acid

X. Z. He, J. G. Li (E-mail: laserli@sina.com), X. Y. Zhang. University of Science and Technology Liaoning, China, L. Yan, State Key Laboratory of Metal Material for Marine Equipment and Application, Ansteel Group Research Institute, China

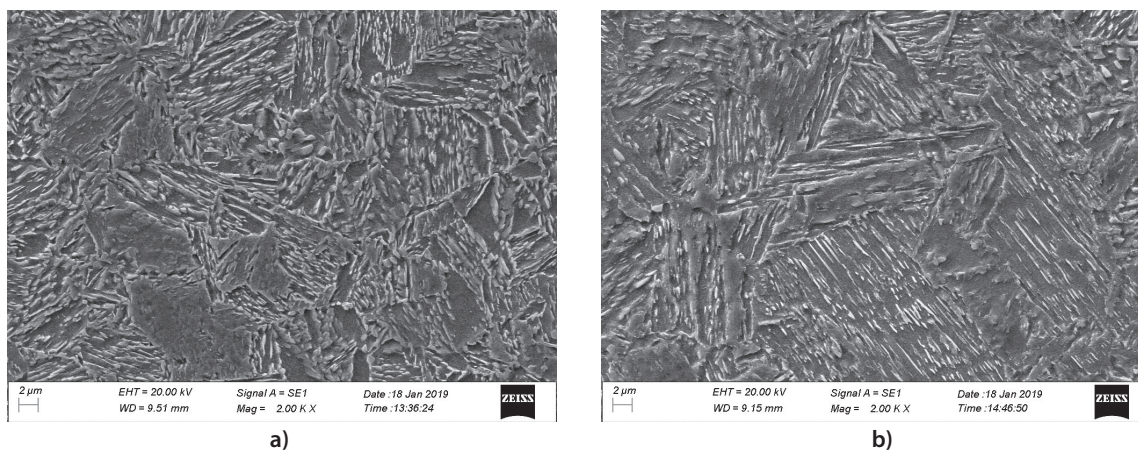


Figure 1 SEM image of experimental steel after different heat treatments: (a) SEM image of T1; (b) SEM image of T2

solution, with two samples. The EBSD samples were ion-polished, and their microstructure and retained austenite distribution were observed on a FEI Nova Nano SEM 450 machine. The retained austenite content of the samples was measured on an X'PERT PRO X-ray diffractometer. A 0,5 mm thick sample was cut by wire cutting, ground to 30 μm , and then subjected to double-spray thinning treatment. The microstructure before and after stretching was observed under a JEOL JEM-2010 UHR transmission electron microscope (TEM).

RESULTS AND DISCUSSION

Microstructure

Figure 1 shows SEM topographies generated by the two heat-treatment processes. Figure 1(a) shows the microstructure of test steel T1 after 830 $^{\circ}\text{C}$ quenching + 640 $^{\circ}\text{C}$ tempering. It is clear that the microstructure is mainly composed of ferrite and martensite, the ferrite is irregularly distributed between the lath martensite, and the retained austenite is distributed between the ferrite and martensite grain boundaries. Figure 1(b) shows the microstructure of the T2 test steel after 830 $^{\circ}\text{C}$ quenching + 720 $^{\circ}\text{C}$ intercritical annealing + 640 $^{\circ}\text{C}$ tempering. During critical annealing, the martensite/bainite portion is austenitized during the heating process. During subsequent cooling, no depletion of C, Mn, or Ni

occurs in austenitized martensite/bainite, and the shape maintains the original basic lath-shape organization, called critical ferrite. It is evident from Figure 1(b) that the test steel consists of martensite/bainite + critical ferrite + a small amount of retained austenite.

The austenite distribution of test steels T1 and T2 was analyzed by EBSD. As shown in Figure 2, the blue region is austenite, the retained austenite is in the shape of a block and a long film, and the retained austenite grains are very fine and dispersed in martensite/bainite and ferrite slats. The retained austenite contents of t1 and t2 were 1,37 % and 0,13 %, respectively. The retained austenite is dispersed in the lath structure, and its microstructure is fine and stable. The finely dispersed residual austenite transforms into martensite, and the martensite formed is a hard phase; martensite particles can provide more second-phase interface, which is beneficial to the formation of dimples, and hence, improves crack extension energy during impact. During crack propagation, the fine and dispersed residual austenite can split the crack and absorb more energy.

Due to the small size of the retained austenite grains in the matrix structure, the volume fraction of retained austenite in the test steel under the two heat-treatment processes was quantitatively analyzed by XRD. As a result, as shown in Figure 3, the austenite contents of T1 and T2 were found to be 20,8 % and 18,1 %, respectively.

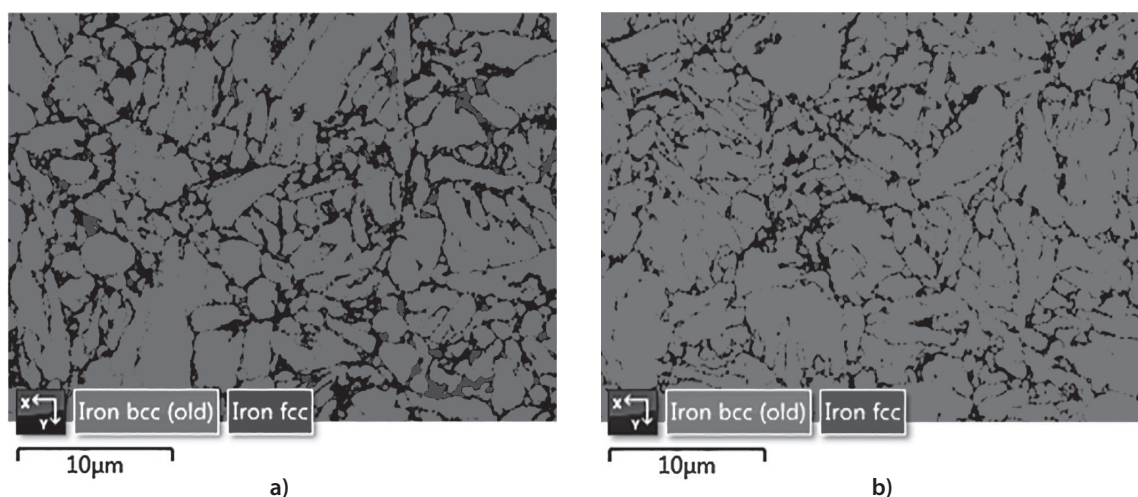


Figure 2 EBSD image of test steel after different heat treatments: (a) EBSD image of T1; (b) EBSD image of T2.

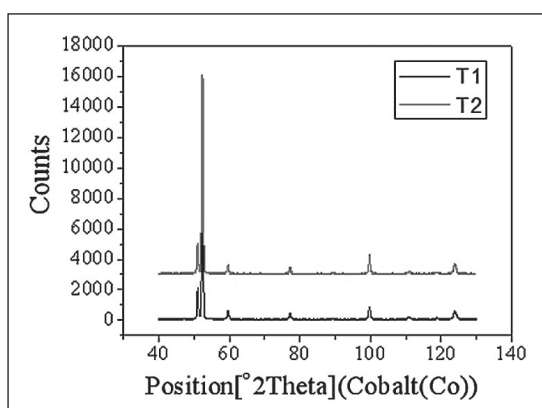


Figure 3 XRD patterns of T1 and T2

Residual austenite grain size and C content under QIT process

Y.Q. TIAN, et al. [7] believe that stable retained austenite can effectively improve the low-temperature toughness of steel and that the size, morphology, and C content of retained austenite will affect its stability. As shown in Figure 4, the retained austenite was 90 – 140 nm wide, 500 – 1 500 nm long, less than 500 nm in width, and was distributed between the slats in a film shape and a lamellar shape. The film-like retained austenite existing between lath martensite has high stability because the carbon content of the film-like retained austenite is high-

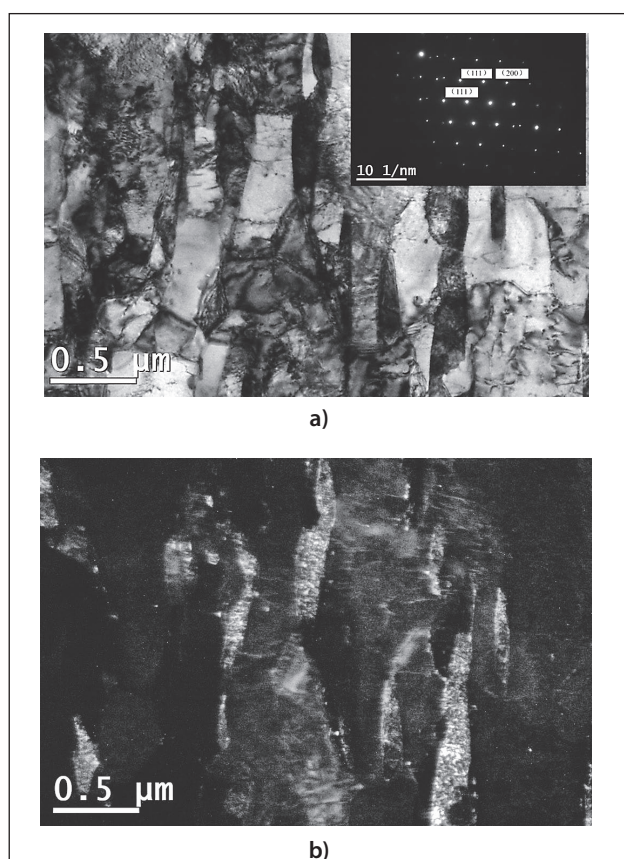


Figure 4 T2 test steel retained-austenite TEM bright-field image, dark-field image, and SAED pattern: (a) bulk and film-like retained austenite; (b) dark-field image.

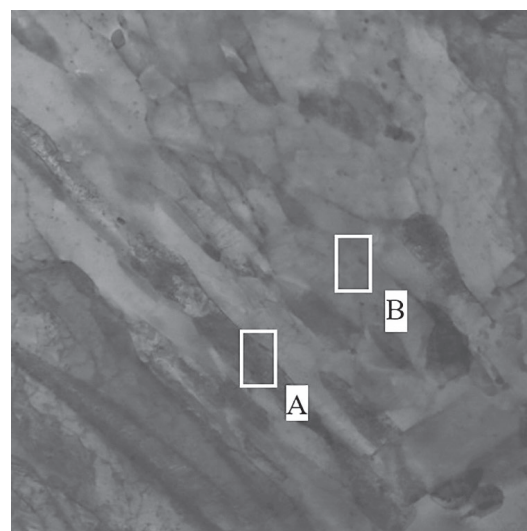


Figure 5 TEM image of T2 test steel

er than that of the block and its thermodynamic and mechanical stability are higher. Under high-stress conditions, it will be partially transformed into martensite, which can greatly improve low-temperature toughness.

Table 1 The area A and B EDS analysis / atom,%

Area	C	Si	Mn	Ni	Cu	Nb	Mo
A	11.85	6.78	15.92	29.58	35.87	0	0
B	6.93	7.66	8.81	31.28	40.90	0	4.42

The C and Mn elements have a stabilizing effect on retained austenite. After the two-phase zone is annealed and tempered, the C and Mn elements are enriched in retained austenite to enhance its stability. In addition, the C content also has an effect on the TRIP effect. To obtain the best TRIP effect, the average C content of retained austenite in TRIP steel should be above 0,95 % (mass fraction) [8, 9]. As shown in Figure 5 and Table 1, the EDS spectrum of the film-like retained austenite of the T2 sample steel was analyzed. The atomic percentage of the C element was 11,85 %, and the mass percentage was 2,71 %, which is higher than the residual austenite C content in ordinary TRIP steel, and the stability is good.

Figure 6 shows a TEM bright-field image and a SAED diffraction pattern at 4 mm from the tensile fracture of the T2 sample. There are a large number of dislocations and similar slats in the structure, no obvious slat characteristics, and less residual austenite content. The austenite is also distributed between the grains in film form. The grain length of the retained austenite before deformation was 500 – 1500 nm, and the width was 90 – 140 nm; 4 mm from the fracture, the retained austenite grain length was about 200 – 300 nm, and the width was less than 40 nm. As the strain increased, the phase transition preferentially occurred in the larger retained austenite grains because the smaller retained austenite grains have high stability and are not prone to phase transformation. During stretching at room temperature, the amount of massive residual austenite gradually decreases, and only a small amount of thin-film residual austenite re-

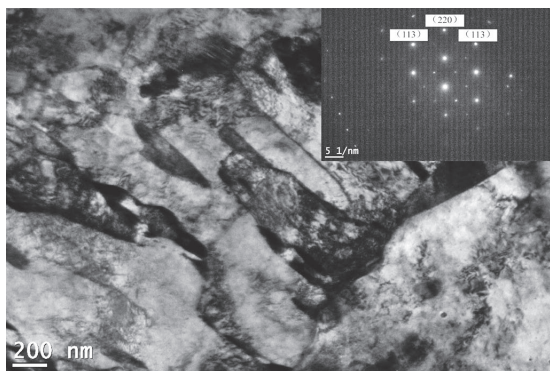


Figure 6 TEM bright-field image and SAED pattern at 4 mm from the tensile fracture of the T2 sample

mains, indicating that the stability of thin-film residual austenite is better than that of massive residual austenite, that phase change is more likely to occur under stress, and that film-like retained austenite has high mechanical stability, which can greatly improve the low-temperature toughness of low-carbon steel.

Mechanical stability of retained austenite

The mechanical stability of the retained austenite is indicative of its ability to resist deformation. There are many ways to evaluate the mechanical stability of retained austenite; this paper uses the approach of calculating the austenite stability coefficient proposed by Sugimoto et al. [10, 11] and expressed in Equation 1:

$$\log f_r = \log f_{r0} - K\varepsilon \quad 1$$

Where f_r is the amount of retained austenite after strain, f_{r0} is the amount of retained austenite before strain, ε is the amount of strain and K is the retained austenite stability coefficient. The expression for K is obtained by manipulation of Equation 1, as shown in Equation 2:

$$K = -\frac{\ln(f_r / f_{r0})}{\varepsilon}, \quad 2$$

The calculated K values for retained austenite mechanical stability were 4,511 for the T1 sample and 2,596 for the T2 sample. The smaller the value of K , the better will be the stability of retained austenite, so that the residual austenite transformation of the T2 sample during stretching was less than that of T1, meaning that the tensile and yield strengths were lower than those of T1. However, due to the high austenite content of the T1 and T2 samples, a large amount of austenite-to-martensite transformation (i.e., the TRIP effect) occurred, and the more stable the retained austenite in steel, the more the work-hardening behavior continues, delaying necking and increasing elongation. In the -40°C impact test, the retained austenite was dispersed and distributed between ferrite and martensite. The retained austenite stabilized between the martensite laths prevented the formation of martensite and ferrite cracks, and the retained austenite improved plastic deformation capability before crack initiation, thereby obtaining higher cracking work and improved low-temperature impact toughness of the test steel.

CONCLUSIONS

In the (quenching + two-phase annealing + 640°C tempering) process, the film-like/lamellar retained austenite had higher stability than the bulk retained austenite. The smaller the grain size of the retained austenite, the higher will be the thermal stability. The C content in the retained austenite contributes to its stability. The stability of the retained austenite between the slats is greater than that of retained austenite at other locations.

Acknowledgements

This work was supported by the State Key Laboratory of Marine Equipment and Applied Metal Materials and the University of Science and Technology Liaoning Joint Funding Project.(No.SKLMEA-USTL-201701).

REFERENCES

- [1] X.X. Li, R.Q. Na, Z.C. Meng. An Analysis on Application and Trend of Low-Alloy Steel in Shipbuilding and Offshore Engineering Industry [J]. Journal Of Iron And Steel Research International 18(2011), 827-830.
- [2] M.M. Linares, A. Jenifer, Iván D, et al. Marine atmospheric corrosion of carbon steels [J]. Revista de metalurgia 51(2015)2.
- [3] D.D.N. Singh, S. Yadav, J.K. Saha. Role of climatic conditions on corrosion characteristics of structural steels [J]. Corrosion Science 50(2008)1, 93-110.
- [4] I. Diaz, H. Cano, P. Lopesino, et al. Five-year atmospheric corrosion of Cu, Cr and Ni weathering steels in a wide range of environments [J]. Corrosion Science 141(2018), 146-157.
- [5] J. Verma, R.V. Taiwade. Effect of welding processes and conditions on the microstructure, mechanical properties and corrosion resistance of duplex stainless steel weldments-A review [J]. Journal Of Manufacturing Processes 25(2017), 134-152.
- [6] H.C. Ma, Z.Y. Liu, C.W. Du, et al. Stress corrosion cracking of E690 steel as a welded joint in a simulated marine atmosphere containing sulphur dioxide [J]. Corrosion Science 100(2015), 627-641.
- [7] Y.Q. Tian, G. Tian, X.P. Zheng, et al. C and Mn Elements Characterization and Stability of Retained Austenite in Different Locations of Quenching and Partitioning Bainite Steels(in Chinese)[J]. Acta Metallurgica Sinica 55(2019)3, 332-340.
- [8] D.V. Edmonds, K. He, F.C. Rizzo, et al. Quenching and partitioning martensite—A novel steel heat treatment[J]. Materials Science and Engineering A (Structural Materials: Properties, Microstructure and Processing) 438(2006), 25-34.
- [9] D.Z.S. Van, L. Zhao, S.O. Kruijver, et al. Thermal and mechanical stability of retained austenite in aluminum-containing multiphase TRIP steels[J]. ISIJ international 42(2002)12, 1565-1570.
- [10] K. Sugimoto, N. Usui, M. Kobayashi, et al. Effects of volume fraction and stability of retained austenite on ductility of TRIP-aided dual-phase steels[J]. ISIJ international 32(1992)12, 1311-1318.
- [11] S.K. Liu, J. Zhang. The influence of the Si and Mn concentrations on the kinetics of the bainite transformation in Fe-C-Si-Mn alloys[J]. Metallurgical Transactions A (Physical Metallurgy and Materials, Science) 21(1990)6, 1517-1525.

Note: The responsible translator for language English is associate professor Q.H. Pang - University of Science and Technology Liaoning, China.